SYNCHRONIZATION CRITERIA OF LINE-START PERMANENT MAGNET SYNCHRONOUS MOTORS: A REVISIT

A. Chama, A.J. Sorgdrager R-J Wang *

* *Dept of Electrical & Electronic Engineering, Stellenbosch University, Private Bag X1, Matieland 7602, South Africa E-mail: chama@aims.ac.za, ajsorgdrager@gmail.com, rwang@sun.ac.za*

Abstract: A main challenge in designing a line-start permanent magnet synchronous machine (LS-PMSM) is the synchronization analysis and determination. Often the use of time-consuming transient time-step finite element (FE) simulations is unavoidable in the design process. An attractive alternative is to use an analytical synchronization model, which is efficient and can be included in an optimization procedure. However, the implementation of the energy based synchronization criteria is complex as there is little explanation of mathematical principles and function estimations in literature. This paper attempts to revisit and evaluate the viability of the analytical synchronization model.

Key words: Line-start motor, permanent magnet machine, synchronization, analytical modelling, finite element method, transient performance

1. INTRODUCTION

When designing a LS-PMSM, both steady-state and transient operations must be considered. This differs from common synchronous machines design approaches, where usually only the steady-state operation is considered, as a power electronic drive is used for precise motion control. The self-starting capability is a key advantage and also a design challenge for LS-PMSMs. Traditionally, the design of an LS-PMSM starts from the steady-state performance optimization. When the optimum design has been realized, the synchronization capability of the machine is then verified for the specific application. The design is considered a success if the machine synchronizes, otherwise, another design iteration is necessary.

There is extensive published work on steady-state design and optimization of LS-PMSMs using both classical machine theory or finite element method (FEM). For validating the synchronization performance of LS-PMSMs, the more favored approach is the use of transient time-step FEM simulations. However, this verification method is computationally expensive thus limiting the possibility for designers to incorporate it into an optimization procedure.

The use of an analytical synchronization model has been proposed by researchers such as Honsinger [1], Miller [2], Rahman [3–5] and Soulard [6]. This energy based synchronization criteria model is very efficient and can be readily implemented as part of an optimization framework, which will minimize the use of costly transient time-step FEM simulations. However, the implementation of the energy based synchronization criteria from past literature can be difficult to follow and repeat as authors used different notations and symbols for the same parameters without clearly defining them. There is also a lack of clear explanation of mathematical principles and function estimations applied to determine certain key parameters, which are required to determine an accurate synchronization conformation.

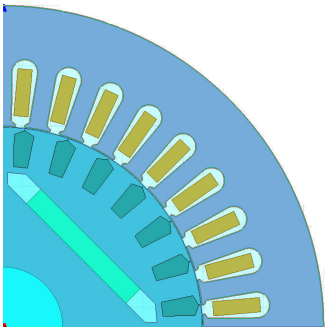

Figure 1: LS PMSM with interior radial flux PMs

The aim of this paper is to revisit the energy based synchronization criteria as presented in past literature. In doing so a detailed explanation of each component and implementation steps of the critical synchronization criteria for a LS-PMSM can be clarified. To check the viability of the analytical approach, the analytically determined synchronization status for several LS-PMSMs is further verified by comparing it to results obtained from transient time-step FEM simulations.

2. ANALYTICAL SYNCHRONIZATION CRITERIA

In this section, the analytical torque equations of a LS-PMSM based on classical electric machine theory are first presented, based on which an analytical synchronization model is then formulated and implemented. The relevant computational aspects are also described.

As shown in Fig. 1, a LS-PMSM has a hybrid rotor, which contains both cage winding and PMs. The transient state of a LS-PMSM machine is rather complex as the behavior of the machine is affected by a number of torque components as illustrated in Fig. 2, where T_c, T_b and T_s stand for cage torque, braking torque and synchronous torque respectively. According to [1, 5, 7], these torque

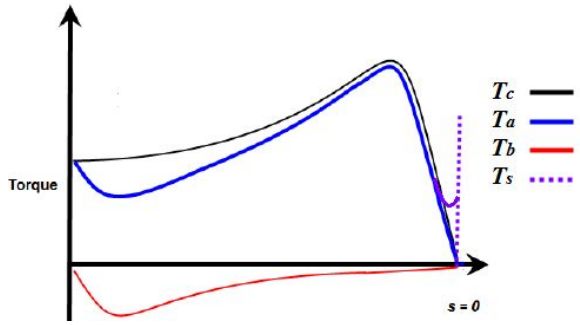

Figure 2: LS-PMSM torque components as a function of slip

components can be expressed as functions of the slip s and load angle δ in radians as follows:

$$T_b(s) = \frac{mpE_0^2R_1}{\omega_s} \cdot \frac{\left[R_1^2 + (1-s)^2X_q^2\right](1-s)}{\left[R_1^2 + (1-s)^2X_qX_d\right]^2} \tag{1a}$$

$$T_c(s) = \frac{mp}{\omega_s} \cdot \frac{sR_2'V_{ph}}{(sR_1 + c_1R_2)^2 + (sX_1 + c_1X_2)^2} \tag{1b}$$

$$T_s(\delta) = T_{s_0} + T_{s_1}\sin\delta + T_{s_2}\sin 2\delta + T_{s_3}\cos\delta + T_{s_4}\cos 2\delta \tag{1c}$$

where the components of T_s are the coefficient of the trigonometrical functions in the explicit formulation of T_s, see (A.10), and $c_1 = \dfrac{1+X_1}{X_m}$. From (A.7)-(A.9), the average and instantaneous torques can be defined as follows:

$$T_a(s) = T_c(s) + T_b(s) \text{ and } T_i(s,\delta) = T_s(\delta) + T_a(s) - T_l(s)$$

with $T_l(s) = T_{\text{rated}}(1-s)^2$ being the load torque; T_{rated} is the rated torque of the machine at synchronous speed. The instantaneous torque T_i follows the equation of motion in the $s-\delta$ plane, i.e.

$$-\frac{J\omega_s^2}{p} \times s\frac{\mathrm{d}s}{\mathrm{d}\delta} = T_i(s,\delta) \tag{2a}$$

The eqn. (2a) is a nonlinear ordinary differential equation and can be solved by the implicit Runge-Kutta-Felhlberg method. To implement the method, (2a) can be first written in the form:

$$\frac{\mathrm{d}s}{\mathrm{d}\delta} = -\frac{p}{J\omega_s^2 s}T_i(s,\delta) = f(s,\delta) \tag{2b}$$

Starting with an initial condition $s_0 = s(0) = 1$, the six-stage coefficient K_j is evaluated at each i^{th} iteration:

$$K_j = hf(s_i + \sum_{n=1}^{j-1}\gamma_{jn}k_n, \delta_i + \alpha_j h_j)\,,, \quad j = 1,\cdots,6,$$

where γ_{jn} and α_j are the coefficients of Butcher table for the Fehlberg's $4-5$ order method. Next the forth and firth order Runge-Kutta approximate solutions y_{i+1} and k_{i+1} of problem (2b) are computed. The local discritization error is then expressed as:

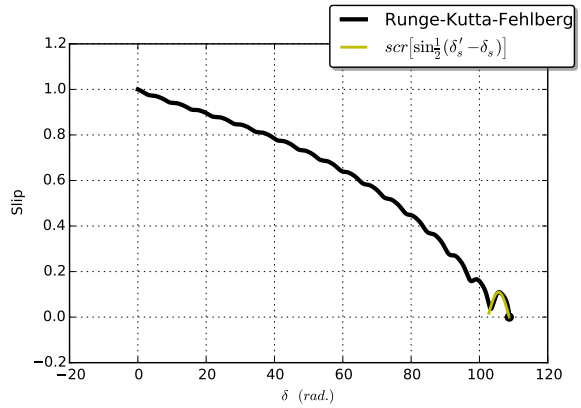

Figure 3: Slip as a function of the load angle: solution by an implicit iterative Runge-Kutta-Fehlberg method.

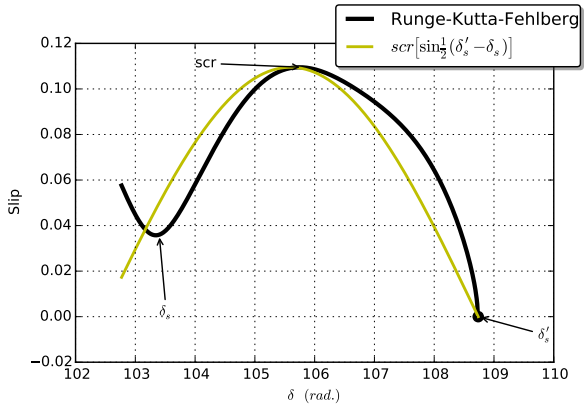

Figure 4: Slip-δ function in the synchronization region

$$\tau = \frac{|y_{i+1} - z_{i+1}|}{h_{i+1}}$$

If τ it greater than the set tolerance in the implementation, then the approximation is accepted; else a new step size is chosen for a better convergence. The program terminates if the value $s = 0$ is found within a tolerance less than 10^{-10}.

Figure 3 shows the slip as a function of the load angle obtained by the numerical implementation of the Runge-Kutta-Fehlberg method. Figure 4 compares this implementation with the approximation of the synchronization region proposed in [5]. Clearly, there exists a good agreement between the two approaches. However, to the contrary of [5], where the proof and error estimate have been omitted, the proposed approximation is well known to have at least a forth order of convergence. Choosing the mesh size h to be small enough would allow us to reach the critical synchronization state with a very small relative error.

One of the advantage of the direct resolution of the PDE's (2) is that it allows in certain context to easily recognize the synchronization capability of the machine without deeper treatment of the problem. Figures 5 and 6 show clear indication of non-synchronized machine, whereas Figure 7 shows that the machine does indeed synchronize to operate at rated conditions of the machine.

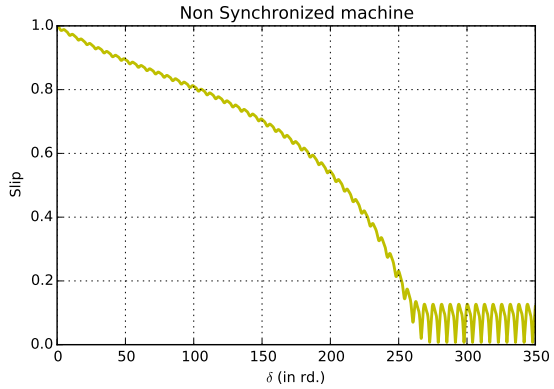

Figure 5: Slip-δ curve of a non-synchronized machine.

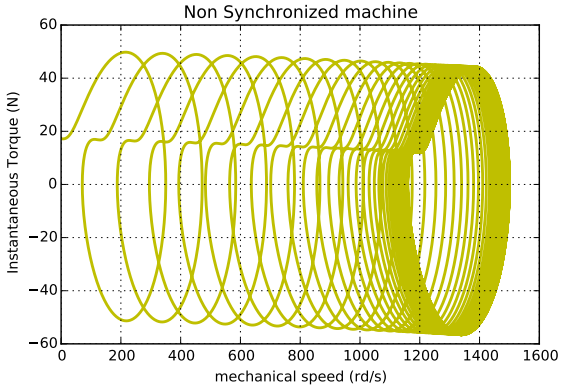

Figure 6: Instantaneous torque of a non-synchronized machine.

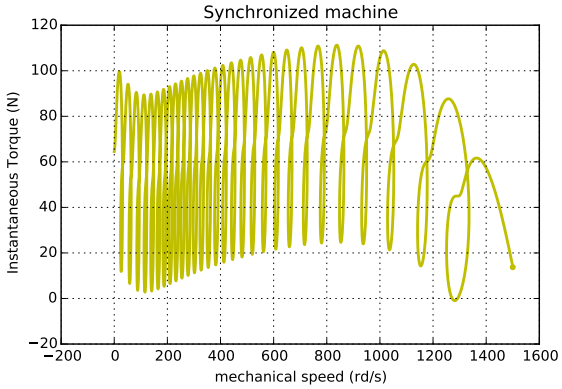

Figure 7: Instantaneous torque of a synchronized machine.

2.1 *Synchronization Conditions*

The critical synchronization state of the machine is determined within the domain $[\delta_s, \delta'_s]$ [7], which is depicted in Fig. 4. The necessary kinetic energy E_k to pull the motor into synchronization is evaluated from the critical slip $s = s_{scr}$ to zero slip, $s = 0$:

$$E_k = \int_{Scr}^{0} -\frac{1}{p} J\omega_s^2 s \, \mathrm{d}x = \frac{1}{2p} J\omega_s^2 s_{scr}^2 \tag{3a}$$

The synchronization energy from point δ_{scr} to δ'_s is

$$E_{syn} = \int_{\delta_{scr}}^{\delta'_s} T_i(s(\delta),\, \delta)\, \mathrm{d}\delta, \tag{3b}$$

where δ_{scr} is the $x-$axis component of the critical point scr.

The machine synchronize for situation when: $E_{scr} \leq E_{syn}$, otherwise it does not synchronize. A flow chart describing the implementation of synchronization criteria as discussed in [5] is shown in Fig. 8.

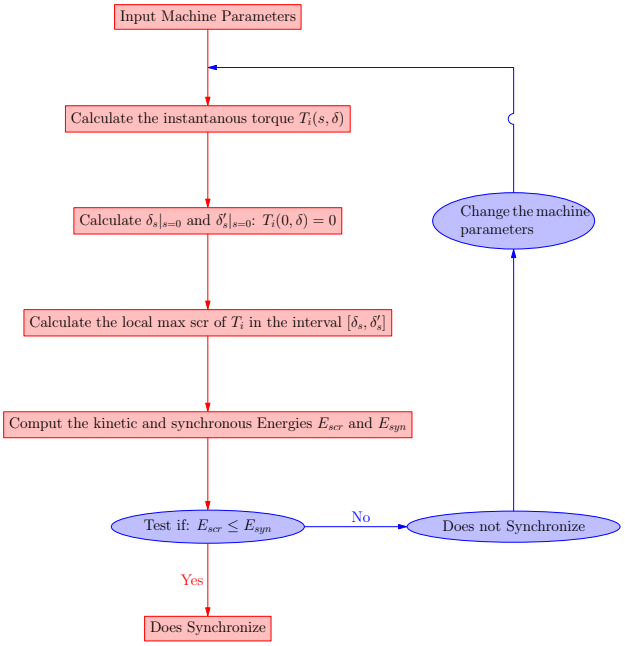

Figure 8: Flow chart describing the implementation of synchronization criteria in [5].

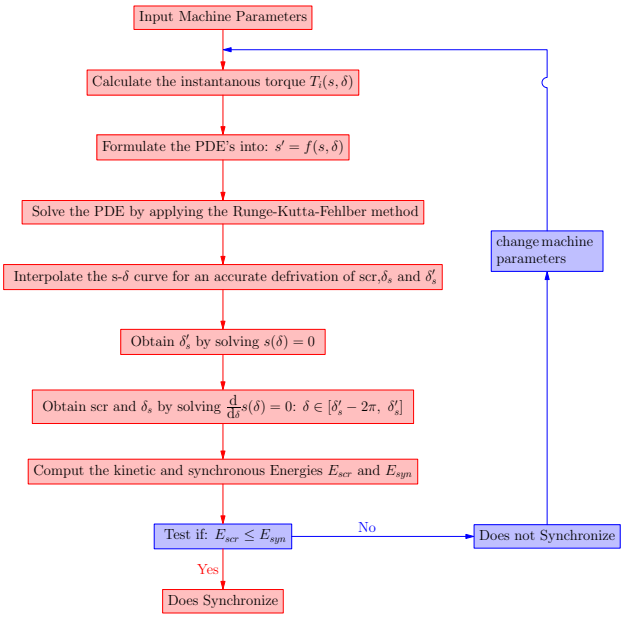

Figure 9: Flow chart describing the implementation of synchronization criteria using the proposed approach.

To evaluate the integrals (3a) and (3b), δ'_s need to be found by solving the equation $T_i(0,\delta) = 0$, the existence of solutions of which can be analyzed from a graphical representation of the instantaneous torque $T_i(0,\delta)$, see

Fig. 10. To obtain the critical slip the equation $T_i(s, \delta'_s - \pi) = 0$ has to be solved, see Figure 11. Note that s_{cr} must be the closest local maximum of the $s - \delta$ function to the origin $s = 0$ and δ'_s the second x-intercept of the curve of T_i.

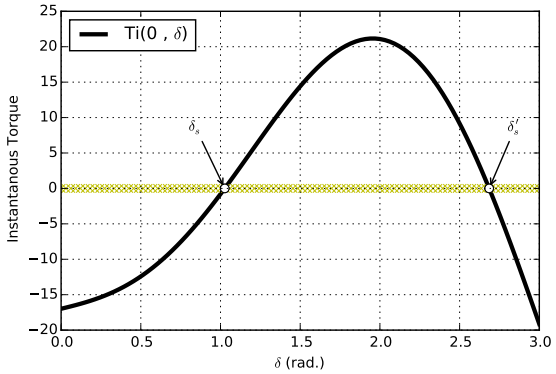

Figure 10: Instantaneous Torque at $s = 0$, as a function of the load angle.

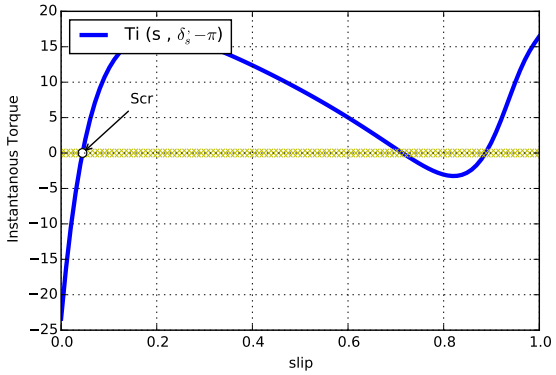

Figure 11: Local maximum s_{cr}, of the instantaneous torque.

3. VALIDATION OF SYNCHRONIZATION MODEL

In this section the synchronization criteria formulated in section 2 is verified using a number of different LS-PMSM designs. The basic specifications for all the designs are given in Table 1. In addition, the machines' rotor diameter, stack length and stator slot are all identical. The differences among these candidate designs are mainly in PM array topologies and rotor slot shapes. Figure 12 illustrates 4 of a total of 13 candidate designs.

For verification, ANSYS' Maxwell software suite that contains both a 2D FEM simulator and an analytical machine model solver (RMXprt) is used. A load equation emulating a fan load is defined for the simulation, which provides a rated load torque at synchronous speed with the inertia as in Table 1.

3.1 Analytical comparison

To accurately calculate the critical slip of a LS-PMSM, the analytical torque curves for the machine is required. RMXprt can produce the required torque curves for each of

Table 1: Machine and load specifications

Specification	Value
Rated output power, kW	2.2
Rated voltage (line-to-line), V	525
Rated speed, rpm	1500
Rated torque, Nm	14
Frame size	100L
Load type	Fan
Load inertia, kg.m^2	0.15
Steady state performance	IE4

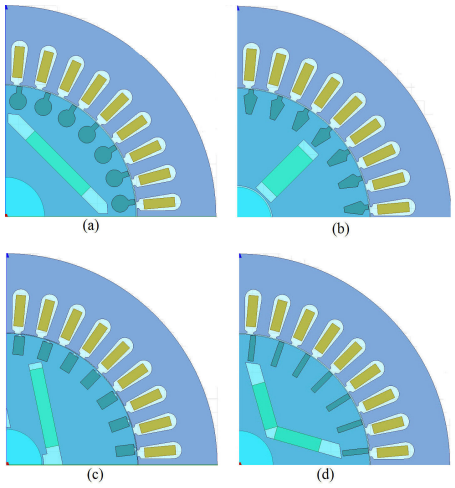

Figure 12: Rotor topology used for verification designs: a) Radial Flux, b)Spoke-type, c)Asymmetric Flux, d) V-type

the candidate designs as well as the key equivalent circuit parameters. However, the exact equations employed by RMXprt torque calculations are unknown. To validate the torque equations (A.7) to (A.9) used in the study, the parameters obtained from RMXprt are used as inputs to reproduce the torque curves from RMXprt. The required RMXprt parameters for a total of 13 designs are listed in Table 2 (See the Appendix for detailed definition of each parameter in the table).

For each machine $T_c(s)$, $T_b(s)$, $T_a(s)$ and $T_s(\delta)$ were created and compared with those from RMXprt. Figures 13 to 16 compare the torque plots for the candidate design 6. Clearly there is a good correlation between the

Table 2: RMXprt output parameters

	E_0	X_d	X_q	R_1	R'_2	X_1	X_2
1	171.20	33.25	99.53	6.63	3.99	3.07	1.80
2	171.20	33.25	99.53	6.63	2.1	3.07	1.80
3	232.40	50.08	107.21	6.64	4.11	4.29	1.52
4	218.36	51.03	107.55	9.91	4.11	4.63	1.52
5	247.86	51.53	159.32	9.92	2.35	4.22	1.45
6	241.26	55.22	153.49	7.61	3.22	4.19	2.43
7	224.94	37.11	99.72	3.69	2.45	3.06	1.98
8	189.60	37.70	101.37	8.42	2.74	3.96	1.85
9	227.41	39.07	106.88	8.42	2.85	3.95	2.64
10	233.03	35.99	172.59	9.66	1.97	6.06	0.832
11	166.92	37.14	164.94	9.30	3.35	5.61	1.56
12	187.65	33.63	99.75	8.42	2.89	3.92	2.06
13	181.16	28.32	101.37	8.43	2.47	3.92	1.63

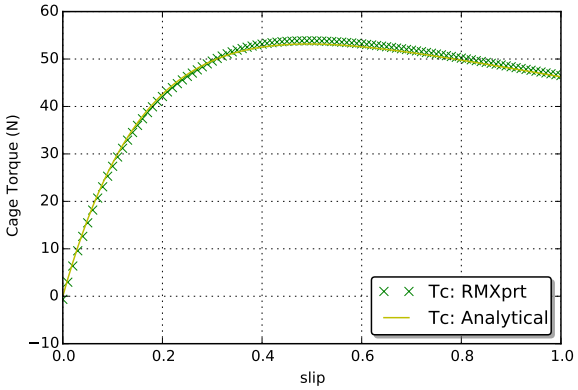

Figure 13: Torque curve comparison of T_c

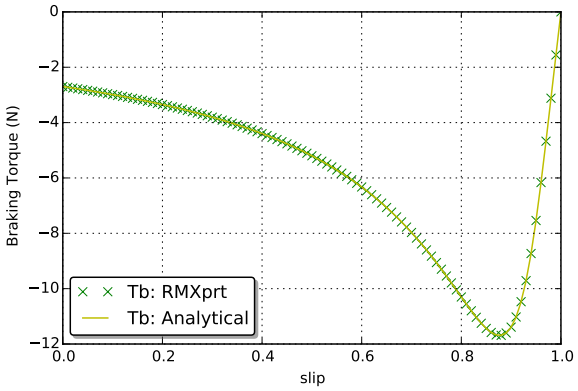

Figure 14: Torque curve comparison of T_b

results from equations (A.7) to (A.9) and RMXprt. The same was found to be true for the remaining 12 candidate designs, which means that these torque equations of LS-PMSMs can be used to solve eqn. (2b).

3.2 Synchronization comparison

In this section the synchronization capabilities of all 13 candidate designs are inspected with the proposed fan load. The analytical synchronization criteria model is applied to each candidate design and the results are verified by using ANSYS' Maxwell 2D transient FEM solver.

In 2D FEM, a load equation can be include in the transient time-step simulation set-up. This was done by defining the

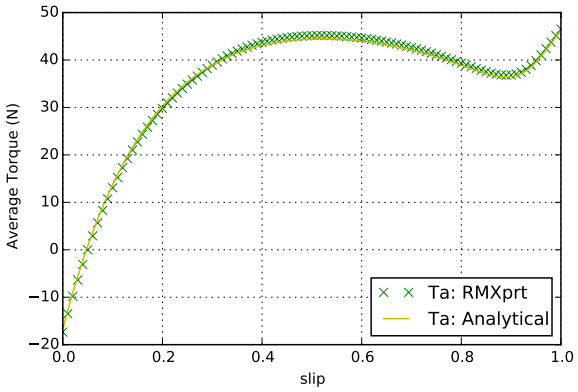

Figure 15: Torque curve comparison of T_a

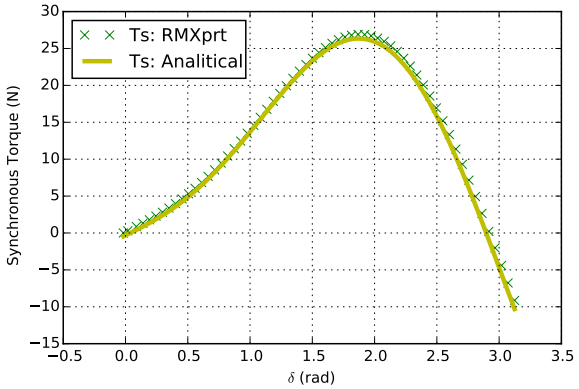

Figure 16: Torque curve comparison of T_s

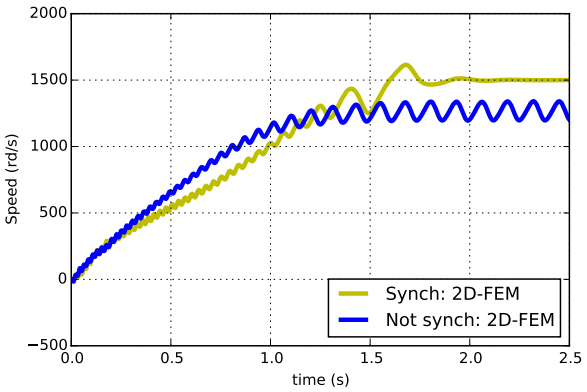

Figure 17: Synchronized vs non-synchronized FEM simulation representations, where design 1 in blue, design 2 in yellow.

load equation as $T_l = 14(1-(157.08-\omega_r)/157.08)^2$ with ω_r referring to the rotors angular velocity in rad/s. The system inertia (J_l) was set at $0.15\,kg.m^2$ and a time-step of $1\,ms$ was used in the analyses. Using the results from the simulations both speed vs. time and instantaneous torque vs. speed graphs are compiled for each candidate design. Figure 17 represents two cases (designs 1 and 2) obtained from the simulation results. The simulation results are interpreted as follows:

- A machine is seen as synchronized once the rotational speed settles at 1500 rpm (yellow line);
- A machine is seen as not synchronized when the rotational speed oscillates at a point below 1500 rpm (blue line).

Figures 18 and 19 are the instantaneous torque vs. speed plots for the two cases. It can be seen that it closely resembles that of Figures 6 and 7 in Section 2 that was obtained using the proposed analytical approach.

The comparison for all the candidate designs is presented in Table 3. The synchronization state of a design is indicated under the method used. The first coulomb from the right states if the result of the proposed method matches that of ANSYS Maxwell 2D FEM. From the table it is clear that a 100% match was achieved.

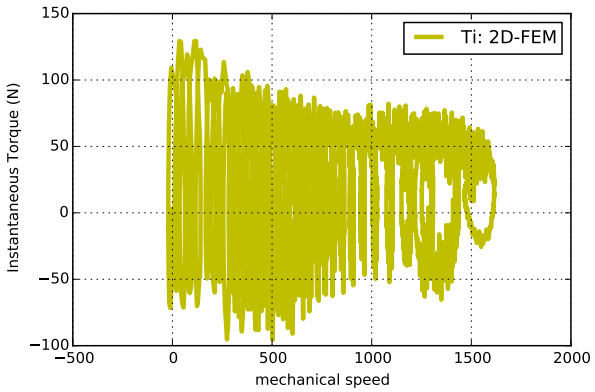

Figure 18: Torque vs speed characteristics obtained from FEM

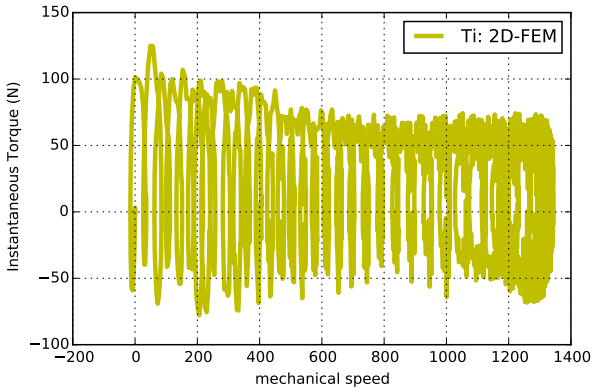

Figure 19: Torque vs speed characteristics obtained from FEM (design 1).

4. CONCLUSION

This paper revisits the energy based synchronization criteria as presented in past literature. An improved and more consistent approach for the study of synchronization by using an energy based synchronization criteria model has been presented. Using an implicit non-linear solver, we have shown how to determine the $s - \delta$ plane function, which can then be used to evaluate the state of synchronization. Despite the simplicity of the algorithm it provides highly accurate result with a large order of convergence. Indeed even the most popular numerical solvers such as the finite element method rarely can provide a second order of convergence, whereas the algorithm used in our case has five order of convergence.

The new approach was verified by means of comparison against 2D FEM transient time-step simulation and an alternative analytical LS-PMSM machine simulation tool. Results proved to compare well and as a result the proposed method can be deemed valid for the use of synchronization estimation during the design of LS-PMSMs. It does however still require experimental validation. This can be done by implementing the proposed method during the design of LS-PMSM in future work and as a result also limit the use of time-step simulations and decreasing design optimization time.

Table 3: Verification results

ID	Synchronize?	2D FEM	Analytical	Match
1	Synchronize?	no	no	✓
2	Synchronize?	yes	yes	✓
3	Synchronize?	yes	yes	✓
4	Synchronize?	no	no	✓
5	Synchronize?	no	no	✓
6	Synchronize?	yes	yes	✓
7	Synchronize?	yes	yes	✓
8	Synchronize?	yes	yes	✓
9	Synchronize?	no	no	✓
10	Synchronize?	no	no	✓
11	Synchronize?	no	no	✓
12	Synchronize?	no	no	✓
13	Synchronize?	no	no	✓

REFERENCES

[1] Honsinger, V.B., ”Permanent magnet machines: asynchronous operation,” *IEEE Trans on Power Apparatus and Systems*, PAS-99(4): 1503-1509, July 1980.

[2] Miller, T.J.E., ”Synchronization of line-start permanent magnet AC motors,” *IEEE Trans on Power Apparatus and Systems*, PAS-103(7): 1822-1828, July 1984.

[3] Rahman, M.A., Osheiba, A.M., Radwan, T.S., ”Synchronization process of line-start permanent magnet synchronous motors”, *Electric Machines and Power Systems*, 24(6):77-592, 1997.

[4] Isfahani, A.H., Vaez-Zadeh, S., Rahman, M.A., ”Evaluation of synchronization capability in line start permanent magnet synchronous motors,” *IEEE International Electric Machines and Drives Conference (IEMDC)*, pp.1346-1350, 15-18 May 2011.

[5] Rabbi, S.F., Rahman, M.A., ”Critical criteria for successful synchronization of line-start IPM motors ”, *IEEE Journal of Emerging and Selected Topics in Power Electronics* , 2(2):348-358, June 2014.

[6] Soulard, J., Nee, H.P., ”Study of the synchronization of line-start permanent magnet synchronous motors,” *Conference Record of the 2000 IEEE Industry Applications Conference*, 1:424-431, 2000.

[7] Tang, R.Y. *Modern Permanent Magnet Machines: Theory and Design*, China Machine Press, Beijing, December 1997.

APPENDIX

List of Symbols

Symbol	definition	unit
c_1	T_c correction factor	
E_o	Back-EMF	V
E_k	Kinetic energy	J
E_{syn}	Synchronization energy	J
E_{scr}	Critical synchronization energy	J
f	Frequency	Hz
J	Inertia	kgmˆ2
J_l/J_s	Load/system inertia	kgmˆ2
l	Load	
m	Stator phases	
p	Pole pairs	
R_1	Stator resistance	Ω
R'_2	Rotor resistance referred	Ω
r	Rotor	
s	Slip	
s_{scr}	Critical slip	
T_a	Average torque	Nm
T_b	Magnetic braking torque	Nm
T_c	Cage torque	Nm
T_i	Instantaneous torque	Nm
T_s	Synchronous torque	Nm
X_1	Stator leakage reactance	Ω
X'_2	Rotor leakage reactance	Ω
X_d/X_q	d-q reactances	Ω
V_{ph}	rms phase voltage	V
δ	Load angle	rad
δ_s	Synchronous load angle	rad
δ'_{scr}	Critical load angle	rad
ω_r	Rotating angular velocity	rad/s
ω_s	Angular frequency	rad/s

Subscripts

scr	Critical
l	Load
r	Rotor

List of Torque Equations

$$X_d = X_1 + X_r d \tag{A.1}$$

$$X_q = X_1 + X_r q \tag{A.2}$$

$$\omega_s = \pi f \tag{A.3}$$

$$X'_2 = \frac{X'_{2d} + X'_{2q}}{2} \tag{A.4}$$

$$X_m = \frac{2 \cdot X_d X q}{X_d + X_q} \tag{A.5}$$

$$c_1 = \frac{1 + X_1}{X_m} \tag{A.6}$$

$$T_b(s) = \frac{mpE_0^2 R_1}{\omega_s} \cdot \frac{\left[R_1^2 + (1-s)^2 X_q^2\right](1-s)}{\left[R_1^2 + (1-s)^2 X_q X_d\right]^2} \tag{A.7}$$

$$T_c(s) = \frac{mp}{\omega_s} \cdot \frac{sR'_2 V_{ph}}{(sR_1 + c_1 R_2)^2 + (sX_1 + c_1 X_2)^2} \tag{A.8}$$

$$T_s(\delta) = T_{s_0} + T_{s_1}\sin\delta + T_{s_2}\sin 2\delta + T_{s_3}\cos\delta + T_{s_4}\cos 2\delta \tag{A.9}$$

$$T_{s_0} = \frac{mpR_1 X_q}{w_s\left(R_1^2 + X_d X_q\right)^2}\left[\begin{array}{l}\left(X_d - X_q\right)\left(\frac{V_{ph}^2}{2} - 1 + E_0^2\right) \\ -E_0^2\left(\frac{R_1^2}{X_q} + X_d\right)\end{array}\right]; \tag{A.10a}$$

$$T_{s_1} = \frac{mpE_0 V_{ph}}{w_s\left(R_1^2 + X_d X_q\right)^2}\left[\begin{array}{l}\left(X_d - X_q\right)\left(R_1^2 - X_d X_q\right) + \\ \left(R_1^2 + X_d X_q\right) X_d\end{array}\right]; \tag{A.10b}$$

$$T_{s_2} = \frac{mpV_{ph}^2}{2w_s\left(R_1^2 + X_d X_q\right)^2}\left[\left(X_d - X_q\right)\left(X_q X_d - R_1^2\right)\right]; \tag{A.10c}$$

$$T_{s_3} = \frac{mpE_0 V_{ph} R_1}{w_s\left(R_1^2 + X_d X_q\right)^2}\left[\left(R_1^2 + X_d X_q\right) - 2X_q\left(X_d - X_q\right)\right]; \tag{A.10d}$$

$$T_{s_4} = \frac{mpV_{ph}^2 R_1}{2w_s\left(R_1^2 + X_d X_q\right)^2}\left[\left(X_d - X_q\right)\left(X_d + X_q\right)\right]; \tag{A.10e}$$